

Nuclear astrophysics and resonant reactions: Exploring the threshold region with the Trojan Horse Method

M. La Cognata*, S. Cherubini*[†], M. Gulino*[‡], L. Lamia*[†],
R. G. Pizzone*, S. Romano*[†], C. Spitaleri* and A. Tumino*[‡]

**Istituto Nazionale di Fisica Nucleare, Laboratori Nazionali del Sud,
Via S. Sofia 62, Catania 95123, Italy*

*†Dipartimento di Fisica e Astronomia “Ettore Majorana”,
Università di Catania, Via S. Sofia 64, Catania 95123, Italy*

*‡Facoltà di Ingegneria e Architettura,
Università degli Studi di Enna “Kore”,
Cittadella Universitaria, Enna 94100, Italy*

Published 25 July 2019

Resonant reactions play an important role in astrophysics as they might significantly enhance the cross section with respect to the direct reaction contribution and alter the nucleosynthetic flow. Moreover, resonances bear information about states in the intermediate compound nucleus formed in the reaction. However, nuclear reactions in stars take place at energies well below ~ 1 MeV and the Coulomb barrier, exponentially suppressing the cross section, and the electron screening effect, due to the shielding of nuclear charges by atomic electrons, make it very difficult to provide accurate input data for astrophysics. Therefore, indirect methods have been introduced; in particular, we will focus on the Trojan Horse Method. We will briefly discuss the theory behind the method, to make clear its domain of applicability, the advantages and the drawbacks, and two recent cases will be shortly reviewed: the $^{19}\text{F}(p, \alpha)^{16}\text{O}$ reaction, which is an important fluorine destruction channel in the proton-rich outer layers of asymptotic giant branch (AGB) stars, and the $^{12}\text{C} + ^{12}\text{C}$ reactions, which play a critical role in astrophysics to understand stellar burning scenarios in carbon-rich environments.

Keywords: Nuclear astrophysics; nuclear reactions; indirect techniques.

1. From Direct Approaches to Indirect Methods. Focus on the THM

Nuclear reactions play a key role in the understanding of astrophysical phenomena as they are responsible of energy production and synthesis of chemical elements

This is an Open Access article published by World Scientific Publishing Company. It is distributed under the terms of the Creative Commons Attribution 4.0 (CC-BY) License. Further distribution of this work is permitted, provided the original work is properly cited.

in a variety of sites such as stars or the early universe. For these reasons, reaction cross sections $\sigma(E)$ have a pivotal role in modelling astrophysical phenomena. However, since typical temperatures can be as low as $\sim 10^6$ K, as in the case of stellar burning in quiescent phases, energies of interest lie well below 1 MeV. For charged particles, they are so low that the Coulomb barrier strongly suppresses fusion cross sections, reaching values as low as nanobarn or picobarn scales. Also, at astrophysical energies, the presence of atomic electrons cannot be neglected as their binding energy is of the same order of interaction energies. Since projectile and target particles are in the form of ions (often not fully stripped) and atoms or molecules, the electron clouds shield the nuclear charges, so the cross sections measured in the laboratory are exponentially enhanced with respect to the case of bare nuclei, by a factor $f(E) = \exp(\pi\eta\frac{U_e}{E})$. Here, U_e is the electron screening potential (see Refs. 1, 2 for a general discussion and Refs. 3, 4, 5 for recent examples). Unfortunately, our present understanding of the electron screening effect is not satisfactory as experimental values of U_e , deduced by comparing extrapolated cross sections with experimental ones, often exceed the theoretical upper limit given by the adiabatic approximation.⁶

The rapid change of cross sections with decreasing energies for charged-particle induced reactions, the uncertainties in magnitude of the cross sections due to the electron screening, the vanishingly small cross sections make measurements at astrophysical energies very challenging, with exponentially large systematic errors. Extrapolation and, in few cases, calculations of the cross sections are often the only way to obtain nuclear cross sections at the relevant energies. For extrapolation, often the astrophysical factor is employed^{1,2}:

$$S(E) = \sigma(E)E \exp(2\pi\eta), \quad (1)$$

where $\eta = Z_1Z_2e^2/\hbar v$ is the Sommerfeld parameter, Z_1 and Z_2 the atomic numbers of the interacting nuclei and v their relative velocity. Since $S(E)$ is a smooth function of the energy, the exponential drop due to Coulomb barrier penetration being divided out, it may allow sounder extrapolation of cross sections from high energies, unless resonances are present.

In the case of resonant reactions, indeed, the factors in Eq. (1) do not compensate for the rapid variations of the cross sections and non-negligible deviations from a smooth trend are to be expected. Therefore, unknown or unpredicted peaks in the astrophysical factor due to excited states of the compound nuclei formed in the fusion reactions might introduce systematic errors in the extrapolation procedure, causing an enhancement the $S(E)$ -factor that may significantly influence astrophysical models, energy production and nucleosynthesis. These apply both to low-energy resonances, prompting the appearance of peaks in the extrapolation regions, and to broad states laying right below the particle decay threshold. Under these conditions, resonances high energy tails may cause the rapid increase of $S(E)$ with decreasing energy, an effect that would be difficult to disentangle from the electron screening enhancement. Moreover, the effect of interference between resonances is

an additional source of uncertainty, contributing to alter our predictions based on simple extrapolations of $S(E)$ from high energy to the Gamow window.

The need of ever more accurate reaction rates, necessary to match the increasingly accurate astrophysical observations, has led to improvements in direct approaches, such as the development of underground laboratories, and the introduction of indirect methods. These have been developed with the aim of bypassing the problems affecting direct measurements at low energies outlined above. In particular, the Trojan Horse Method (THM) (originally introduced in the works;^{9,10} see Refs. 7, 8 for two recent reviews) has been developed to measure $S(E)$ -factors at astrophysical energies for reactions involving charged particles and neutrons (see, for instance, Ref. 11). As we will briefly discuss, this is possible thanks to the suppression of Coulomb and centrifugal barriers, as well as to the possibility to access bare-nucleus astrophysical factors.

The leading idea of THM is to study a $A(a, bB)s$ process performed at energies of several tens of MeV, to deduce the astrophysical factor of the $A(x, b)B$ reaction. The use of relatively large beam energies makes it possible to bypass Coulomb and centrifugal barriers, as well as to avoid electron screening effects. To deduce the $S(E)$ -factor of astrophysical importance, the so-called quasi-free (QF) contribution to the $A(a, bB)s$ cross section has to be disentangled, namely, a participant-spectator mechanism leading to the population of excited states of the intermediate nucleus $F = A + x$, later decaying into $b + B$. A pivotal role is played by particle a , the Trojan Horse (TH) nucleus, which has to show a large $x - s$ cluster structure, to maximise the QF contribution to the $A(a, bB)s$ reaction.

To this purpose, the reaction mechanism sketched in Fig. 1 has to be selected, namely, the participant-spectator process where the TH nucleus undergoes direct breakup into a participant x while the spectator s is emitted without influencing the $A(x, b)B$ sub-reaction. Even if the $A(a, bB)s$ QF reaction is induced at energies well above the Coulomb barrier, astrophysical energies can be reached thanks to the energy paid to break the TH nucleus a and to the $x - s$ intercluster motion. Also negative $A - x$ relative energies can be reached by a careful choice of the kinematic variables,¹² making it possible to explore the subthreshold region.

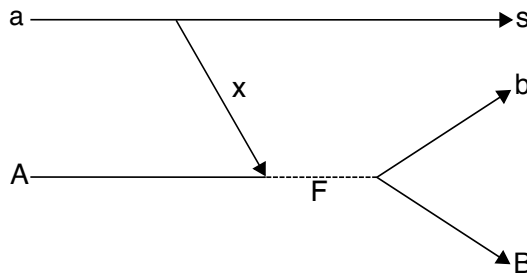


Fig. 1. Sketch of the QF $A(a, bB)s$ reaction, used to transfer a cluster x off the particle a and populate excited states of nucleus F , later decaying to $b + B$.

1.1. The resonant case

The peculiarities of resonant reactions have urged an extension of the THM to account for multiple wave contribution and normalization to the direct data. The original theory based on the plane wave impulse approximation (PWIA), though leading to a very simple relation between the measured $A(a, bB)s$ QF cross section and the $A(x, b)B$ one, supplied only the trend of the astrophysical factor in arbitrary units, making it necessary to determine a scaling constant for each contributing wave 13 (deduced from the comparison with existing direct data at high energies). When many resonances show up in the astrophysical factor, this is a severe problem as normalization would be subject to large uncertainties. This is why extensive theoretical^{14, 15} and experimental^{16, 17} work was carried out allowing us to treat multi-resonance reactions in a more accurate way, named modified R-matrix approach. It makes it possible to account for the half-off-energy-shell (HOES) nature of the $A(x, b)B$ reaction amplitude, due to the fact that the participant cluster x is virtual, and of energy resolution effects that are particularly important in the case of resonant reactions. A simplified version of the theory for narrow resonances is illustrated in Refs. 18, 19; here we will focus on the more general case.

In detail, in the plane wave approximation, the amplitude of the process $a + A \rightarrow b + B + s$ (Fig. 1) is:

$$M^{PWA(prior)}(P, \mathbf{k}_{aA}) = \langle \chi_{sF}^{(0)} \Psi_{bB}^{(-)} | V_{xA} | \varphi_a \varphi_A \chi_{aA}^{(0)} \rangle, \quad (2)$$

where $P = (\mathbf{k}_{sF}, \mathbf{k}_{bB})$ is the six-dimensional momentum describing the three-body system s , b and B . $\chi_{aA}^{(0)} = \exp(i\mathbf{k}_{aA} \cdot \mathbf{r}_{aA})$, $\chi_{sF}^{(0)} = \exp(i\mathbf{k}_{sF} \cdot \mathbf{r}_{sF})$, \mathbf{r}_{ij} and \mathbf{k}_{ij} are the relative coordinate and relative momentum of i and j nuclei, $\Psi_{bB}^{(-)}$ is the wave function of the fragments b and B in the exit channel, $F = b + B$, V_{xA} is the interaction potential of x and the target nucleus A , φ_a and φ_A are the bound state wave function of nuclei a and A , respectively. Even if plane wave approximation is very simple, it is well known that it makes it possible to accurately reproduce the trend of the direct cross section, while the deduced absolute value can be significantly different.²⁰ Assuming that the reaction yield is dominated by resonances and introducing back particle spins, the plane wave amplitude from which the THM cross section is calculated is given by Refs. 7, 15:

$$\begin{aligned} & M^{PWA(prior)}(P, \mathbf{k}_{aA}) \\ &= (2\pi)^2 \sqrt{\frac{1}{\mu_{bB} k_{bB}}} \varphi_a(\mathbf{p}_{sx}) \sum_{J_F M_F j' l' m'_j m_l m'_l m_x} i^{l+l'} \langle j m_j l m_l | J_F M_F \rangle \\ & \times \langle j' m_{j'} l' m_{l'} | J_F M_F \rangle \langle J_x M_x J_A M_A | j' m_{j'} \rangle \langle J_s M_s J_x M_x | J_A M_A \rangle \\ & \times \exp[-i\delta_{bB}^{hs}] Y_{l m_l}(-\hat{\mathbf{k}}_{bB}) \sum_{\nu\tau=1}^N [\Gamma_{\nu b B j l J_F}]^{1/2} [\mathbf{A}^{-1}]_{\nu\tau} Y_{l' m'}^*(\hat{\mathbf{p}}_{xA}) \end{aligned}$$

$$\begin{aligned}
 & \times \sqrt{\frac{R_{xA}}{\mu_{xA}}} [\Gamma_{\nu x A l' j' J_F}(E_{xA})]^{1/2} P_{l'}^{-1/2}(k_{xA}, R_{xA}) \\
 & \times \left(j_{l'}(p_{xA} R_{xA}) [(B_{xA l'}(k_{xA}, R_{xA}) - 1) - D_{xA l'}(p_{xA}, R_{xA})] \right. \\
 & \left. + 2Z_x Z_A e^2 \mu_{xA} \int_{R_{xA}}^{\infty} dr_{xA} \frac{O_{l'}(k_{xA}, r_{xA})}{O_{l'}(k_{xA}, R_{xA})} j_{l'}(p_{xA} r_{xA}) \right). \quad (3)
 \end{aligned}$$

Here, $F = b + B$, μ_{ij} is the $i - j$ reduced mass, r_{ij} is the $i - j$ relative distance, \mathbf{p}_{ij} is the $i - j$ relative momentum in the case of off-energy-shell particles, thus $E_{ij} \neq p_{ij}^2/2\mu_{ij}$ (while \mathbf{k}_{ij} is calculated assuming the particles on-shell), $\delta_{bB l}^{hs}$ is the solid sphere scattering phase shift, R_{xA} the $x + A$ channel radius,

$$B_{xA l'}(k_{xA}, R_{xA}) = R_{xA} \frac{\partial O_{l'}(k_{xA}, R_{xA})}{\partial r_{xA}} \Big|_{r_{xA}=R_{xA}} \quad (4)$$

is the logarithmic derivative as in the R-matrix method,

$$O_{l'}(k_{xA}, R_{xA}) = \sqrt{\frac{k_{xA} R_{xA}}{P_{l'}(k_{xA}, R_{xA})}} \exp[-i\delta_{xA l'}^{hs}] \quad (5)$$

is the outgoing spherical wave, $P_{l'}(k_{xA}, R_{xA})$ is the l' -wave penetrability factor,

$$D_{xA l'}(p_{xA}, R_{xA}) = R_{xA} \frac{\partial j_{l'}(p_{xA}, R_{xA})}{\partial r_{xA}} \Big|_{r_{xA}=R_{xA}} \quad (6)$$

is the logarithmic derivative and $j_{l'}(p_{xA}, R_{xA})$ is the spherical Bessel function, N is the number of the levels included. This is a generalisation of the R-matrix approach because we consider reactions with three particles in the exit channel, where the TH-nucleus a in the initial states carries the transferred particle x , which is off-energy-shell.

The analysis of Eq. (3) shows that $\mathbf{A}_{\nu\tau}$ is the same level matrix as in the R-matrix theory,²¹ thus the same resonance energies and reduced width amplitudes are present in the on-energy-shell (OES) cross section and in the THM one. Therefore, we can reconstruct the OES cross section with no need of extrapolation, taking into account the virtual nature of the transferred particle and energy resolution effects, by unfolding the gaussian response function and the THM cross section. Normalization to direct data can be obtained by introducing in the modified R-matrix the reduced width amplitudes for resonances lying at high energy and accurately known from the literature, even in the case they are populated in different orbital angular momenta. The fact that we can reach zero energy with no Coulomb suppression, in the case of charged-particle induced reactions, is justified by the occurrence of the factor $P_{l'}^{-1/2}(k_{xA}, R_{xA})$ in Eq. (3). Finally, the method can be easily generalized to include the distorted-wave Born approximation (DWBA) (see, for a preliminary work, Ref. 22) or continuum-discretised coupled channel (CDCC) formalisms.¹⁵

These generalisations are particularly important in the case of reactions where no direct data are present, or they show large uncertainties, especially in the case of reactions involving radioactive nuclei and neutrons.

2. The $^{19}\text{F}(p, \alpha)^{16}\text{O}$ Reaction

Fluorine is easily destroyed in the inner layers of stars in proton and α -induced reactions. Therefore, ^{19}F abundance is a very sensitive probe of the physical conditions of the stellar interiors, such as temperature and density, as well as of the mixing mechanisms occurring inside stars. Indeed, during the asymptotic giant branch (AGB) stage of stellar evolution, stars are characterised by a C-O degenerate core surrounded by two shells, the inner one primarily made up of helium, and the outer one still hydrogen rich, alternately burning.²³ These stars undergo repeated mixing episodes (third dredge-up, TDU), and nuclei freshly synthesised in the inner shell are brought to the stellar surface while hydrogen rich material is injected in the deeper layers, owing to partial mixing at the interface between the convective and radiative regions. Here, the so-called ^{13}C pocket forms, which is the main neutron source of the main component of the *s*-process (the slow neutron capture) through the $^{13}\text{C}(\alpha, n)^{16}\text{O}$ reaction (see Ref. 24 and references therein), responsible of the production of about half of the nuclei heavier than iron. ^{19}F is produced in the same layers where the *s*-process is taking place, so its abundance would be a very useful constraint of the models predicting the abundances of heavy elements, provided that exhaustive knowledge of the fluorine destruction cross sections is available.

Due to the mentioned partial mixing,²⁵ fluorine dredged up to the surface can be destroyed in proton induced reactions at the bottom of the convective layer of AGB stars at temperatures $\leq 4 \times 10^7$ K, so it is very important to have exhaustive knowledge of the destruction cross sections to use the fluorine as a sensitive probe. However, the present understanding of fluorine depletion is quite incomplete, possibly owing to a poor accuracy of the cross section of the fluorine destruction processes. Indeed, until 2013 only very old data (dating to 1974) were present below 1 MeV,^{26,27} and only in 2015 a direct measurement reached $E_{c.m.} \leq 300$ keV, where fluorine burning is most efficient at the bottom of AGB convective envelope.²⁸ Moreover, the latest direct data are limited to the α_0 channel, corresponding to the emission of α -particles by ^{20}Ne intermediate system leaving ^{16}O in its ground state. Therefore, an almost linear extrapolation was used to estimate the astrophysical factor below about 500 keV to be adopted in astrophysical models, and this is still the only available extrapolation for other channels involving ^{16}O excited states. This status of the art motivated the beginning of an experimental program aiming at experimentally determine the $^{19}\text{F}(p, \alpha)^{16}\text{O}$ astrophysical factor at the energies of astrophysical interest using the THM, avoiding extrapolation.²⁹⁻³¹

To obtain the $^{19}\text{F}(p, \alpha)^{16}\text{O}$ *S*-factor, the QF $^2\text{H}(^{19}\text{F}, \alpha^{16}\text{O})n$ reaction was studied, exploiting the $d = p + n$ configuration and using deuterons as TH nuclei. By means of Eq. (3), the OES astrophysical factor was deduced from the HOES one,

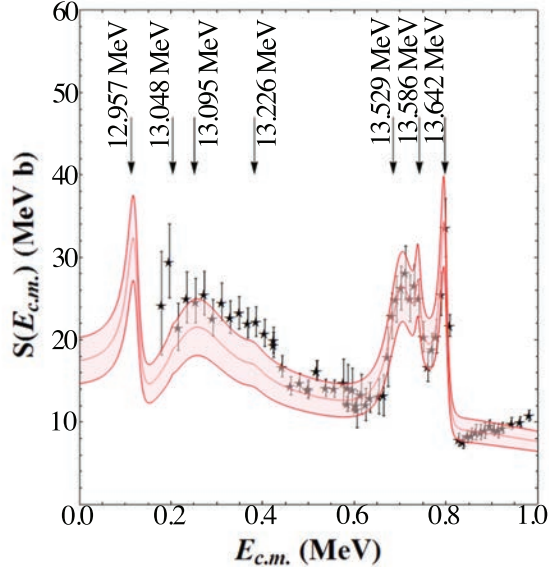


Fig. 2. Comparison of the THM S -factor, including normalisation and statistical errors. (red band) with the most recent direct data (black stars). The arrows mark the ^{20}Ne levels contributing to the $S(E)$ -factor. See text for details.

devoid of energy resolution and electron screening effects. In the first experiment,²⁹ energy resolution prevented us to clearly observe non-isolated ^{20}Ne states, with the risk to perform an incorrect level identification. Yet, this work demonstrated for the first time the presence of a peak lying at 113 keV, namely, well inside the energy region of astrophysical importance. A higher-resolution later work³¹ confirmed the presence of such state while allowing us to perform a better identification of the states showing up in the astrophysical factor. The parallel direct measurements^{27,28} triggered by the seminal work,²⁹ allowed for a more accurate normalization of the THM data (which, as remarked before, are deduced in arbitrary units in the plane wave approximation), and reached very low energies, close the energy range of astrophysical interest, making it possible to indirectly confirm the observation of the 113 keV state through its interference with another resonance lying at higher energies (see Ref. 28 for a more detailed discussion). The comparison between the THM S -factor from Refs. 29–31, given as a red band (where the middle curve displays the recommended astrophysical factor, while the upper and lower limits take into account both statistical and systematic errors), and the direct data from Ref. 27, 28 (indicated by solid stars), is given in Fig. 2.

3. The $^{12}\text{C} + ^{12}\text{C}$ Reactions

$^{12}\text{C} + ^{12}\text{C}$ fusion is a key nuclear reaction in both nuclear physics and astrophysics. Indeed, it has been extensively investigated (see Ref. 32 and references therein) to

understand fusion reaction mechanism, especially because it involves two identical bosons, e.g. to understand the occurrence and origin of the fusion hindrance (see, for instance, Ref. 33). In astrophysics, the $^{12}\text{C} + ^{12}\text{C}$ fusion rate bears a paramount importance in the evolution of massive stars ($M_{\odot} \geq 8$), especially in the case of objects that have left the main sequence. Indeed, as helium burning is over, the stellar core is essentially composed of carbon and oxygen and, since the Coulomb barrier is lowest for the carbon-carbon fusion, when temperatures are high enough (at temperatures greater than 0.4×10^9 K) carbon burning is ignited in the core. $^{12}\text{C} + ^{12}\text{C}$ fusion plays a pivotal role also in the case of explosive phenomena, such as superbursts from accreting neutron stars.³⁴ At present, direct data reach down to about 2.5 MeV center-of-mass energies (experimental data are available at energies as low as 2.1 MeV, but uncertainties are so large that they are not suitable to draw significant astrophysical considerations³²), so extrapolations are necessary to supply the astrophysical factor at the energies of interest, comprised between about 1–2 MeV. Extrapolations are usually performed using the modified astrophysical S -factor³⁵:

$$S^* = E\sigma(E) \exp(2\pi\eta + gE), \quad (7)$$

where $\eta = 13.88 E^{-1/2}$ and $g = 0.46 \text{ MeV}^{-1}$ (the center-of-mass energy E being expressed in MeV).

Owing to the scarcity of the data close to the energy range of astrophysical interest, the sawtooth trend of S^* (probably due to the reduced number of accessible states in the ^{24}Mg compound system due to quantum selection rules in the $^{12}\text{C} + ^{12}\text{C}$ entrance channel, the low reaction Q -value and the pairing gap in the even-even ^{24}Mg system³³), and the incomplete understanding of reaction mechanism (e.g., the role played by fusion hindrance³³), extrapolated S^* values cover more than two orders of magnitude (see Fig. 1 of Ref. 32), making it too inaccurate to draw definite conclusions on many astrophysical scenarios. It is worth noting that in the case of the $^{12}\text{C} + ^{12}\text{C}$ fusion reaction the Coulomb barrier is significantly higher than in the case of proton-induced reactions, so the cross section is already of the order of few nanobarns at $E = 2.5$ MeV; also the electron screening effect may play a significant role, even if data accuracy prevents one to perform any evaluation. Therefore, the application of THM may represent a very important step towards the understanding of the $^{12}\text{C} + ^{12}\text{C}$ fusion mechanism, making it possible to obtain the cross section at astrophysical energies with no need of extrapolation. Also, the use of reactions with three particles in the exit channel makes it possible to reconstruct the reaction Q -value from the energies and the angles of the emitted particles. In this way, we can accurately select the reaction channel of interest, reducing essentially to zero background contribution.

$^{12}\text{C} + ^{12}\text{C}$ fusion was investigated through the THM by selecting the QF contribution to the $^{14}\text{N} + ^{12}\text{C}$ reactions,³⁶ exploiting the observation of the possibility to observe the population of ^{24}Mg excited states by using ^{14}N to transfer a ^{12}C nucleus.³⁷ The experiment, carried out at the *Laboratori Nazionali del Sud, Istituto*

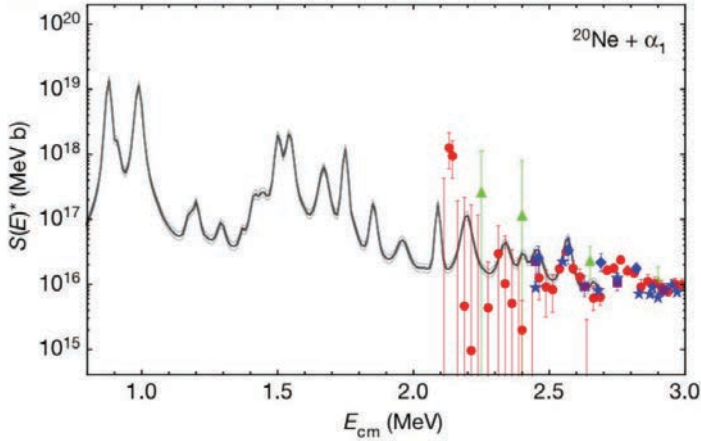


Fig. 3. THM $^{12}\text{C}(^{12}\text{C}, \alpha_1)^{20}\text{Ne}$ modified astrophysical factor S^* (gray band), compared with the available direct data (solid symbols). See text for details.

Nazionale di Fisica Nucleare (Catania, Italy) using a 30 MeV ^{14}N beam delivered the Van de Graff Tandem accelerator, made it possible to extract the cross sections for the $^{12}\text{C}(^{12}\text{C}, \alpha_0)^{20}\text{Ne}$, $^{12}\text{C}(^{12}\text{C}, \alpha_1)^{20}\text{Ne}$, $^{12}\text{C}(^{12}\text{C}, p_0)^{23}\text{Na}$ and $^{12}\text{C}(^{12}\text{C}, p_1)^{23}\text{Na}$ channels, covering the whole energy range of astrophysical interest as well as the energy region above about 2.5 MeV, necessary to normalize the THM S^* factors to the direct ones, in an energy range where the available direct data are less affected by statistical and systematic errors. For the first time, a definite resonant pattern was observed below 2 MeV, well matching the trend of the experimental data in the overlapping energy region. For instance, Fig. 3 shows the $^{12}\text{C}(^{12}\text{C}, \alpha_1)^{20}\text{Ne}$ modified S -factor from 36 obtain by applying Eq. (3), superimposed to the available direct data (filled circles,³⁸ filled squares,³⁹ empty diamonds,⁴⁰ filled stars⁴¹ and filled triangles⁴²) in the same energy region. Clearly, the good agreement that is found in the overlapping energy region is a necessary condition for the application of the THM, and makes it possible to validate the method also in this case. Other approaches, such as those sketched in Refs. 43, 44, presently fail to satisfy such necessary condition, as shown in Ref. 45, demonstrating the robustness of THM.

4. Concluding Remarks

In this work we have discussed about the application of the THM in a particular case, the one of reaction dominated by resonant structures, of great interest for nuclear physics and astrophysics for their implications on nuclear spectroscopy and stellar energetics and nucleosynthesis. We have examined the case of the $^{19}\text{F}(p, \alpha)^{16}\text{O}$ reaction, where deuterons were used to transfer a proton and populate ^{20}Ne excited states, and the $^{12}\text{C} + ^{12}\text{C}$ fusion. In this case, a novel TH nucleus was considered, ^{14}N , used to transfer a ^{12}C nucleus and populate ^{24}Mg excited states. For the first

time many resonances were observed in the astrophysical factors at low-energies, well below the Coulomb barrier, making it possible to deduce high-accuracy reaction rates for astrophysics.

References

1. C. E. Rolfs and W. S. Rodney, *Cauldrons in the Cosmos: Nuclear Astrophysics* (University of Chicago Press, Chicago, 1998).
2. C. Iliadis, *Nuclear Physics of Stars* (Wiley, New York, 2007).
3. M. La Cognata et al., *Phys. Rev. C* **72**, 065802 (2005).
4. A. Rinollo et al., *Nucl. Phys. A* **758**, 146C (2005).
5. A. Tumino et al., *Phys. Lett. B* **705**, 546 (2011).
6. L. Bracci et al., *Nucl. Phys. A* **513**, 316 (1990).
7. R. E. Tribble et al., *Reports on Progress in Physics* **77**, 106901 (2014).
8. C. Spitaleri et al., *Eur. Phys. J. A* **52**, 77 (2016).
9. G. Baur, *Phys. Lett. B* **178**, 135 (1986).
10. C. Spitaleri, *Proceedings of the 5th Winter School on Hadronic Physics: Problems of Fundamental Modern Physics II* (World Scientific, Singapore, 1991).
11. M. Gulino et al., *Phys. Rev. C* **87**, 012801 (2013).
12. M. La Cognata et al., *Astrophys. J.* **777**, 143 (2013).
13. S. Typel et al., *Ann. Phys.* **305**, 228 (2003).
14. A. M. Mukhamedzhanov et al., *J. Phys. G Nucl. Phys.* **35**, 014016 (2008).
15. A. M. Mukhamedzhanov, *Phys. Rev. C* **84**, 044616 (2011).
16. M. La Cognata et al., *Astrophys. J.* **723**, 1512 (2010).
17. M. La Cognata et al., *Phys. Rev. C* **80**, 012801 (2009).
18. M. La Cognata et al., *The Astrophys. J.* **708**, 796 (2010).
19. M. La Cognata et al., *Phys. Rev. Lett.* **101**, 152501 (2008).
20. E. I. Dolinsky, P. O. Dzhamalov and A. M. Mukhamedzhanov, *Nucl. Phys. A* **202**, 97 (1973).
21. A. M. Lane and R. G. Thomas, *Rev. Mod. Phys.* **30**, 257 (1958).
22. M. La Cognata et al., *Nucl. Phys. A* **834**, 658c (2010).
23. M. Busso et al., *Ann. Rev. Astr. Astrophys.* **37**, 239 (1999).
24. O. Trippella and M. La Cognata, *Astrophys. J.* **837**, 41 (2017).
25. M. Busso et al., *Astrophys. J. Lett.* **717**, L47 (2010).
26. C. Angulo et al., *Nucl. Phys. A* **656**, 3 (1999).
27. I. Lombardo et al., *J. Phys. G Nucl. Phys.* **40**, 125102 (2013).
28. I. Lombardo et al., *Phys. Lett. B* **748**, 178 (2015).
29. M. La Cognata et al., *Astrophys. J. Lett.* **739** L54 (2011).
30. M. La Cognata et al., *Astrophys. J.* **805**, 128 (2015).
31. I. Indelicato et al., *Astrophys. J.* **845** 19 (2017).
32. J. Zickefoose et al., *Phys. Rev. C* **97**, 065806 (2018).
33. C. L. Jiang et al., *Phys. Rev. Lett.* **89**, 052701 (2002).
34. R. L. Cooper et al., *Astrophys. J.* **702**, 660 (2009).
35. J. R. Patterson et al., *Astrophys. J.* **157**, 367 (1969).
36. A. Tumino et al., *Nature* **557**, 687 (2018).
37. T. Belyaeva et al., *Phys. At. Nucl.* **65**, 1616 (2002).
38. T. Spillane et al., *Phys. Rev. Lett.* **98**, 122501 (2007).
39. M. G. Mazarakis et al., *Phys. Rev. C* **7**, 1280 (1973).
40. M. D. High et al., *Nucl. Phys. A* **282**, 181 (1977).

41. K. U. Kettner *et al.*, *Z. Phys. A* **298**, 65 (1980).
42. L. Barron-Palos *et al.*, *Nucl. Phys. A* **779**, 318 (2006).
43. A. M. Mukhamedzhanov and D. Y. Pang, arXiv:1806.08828v4 [nucl-th] (2018).
44. A. M. Mukhamedzhanov *et al.*, arXiv:1806.05921v1 [nucl-ex] (2018).
45. A. Tumino *et al.*, arXiv:1807.06148v1 [nucl-ex] (2018).